

The Three-Dimensional CFD Analysis of Flow Behaviors in a Complex Twin-Screw Supercharger

*H.F. Li, J.Y. Tu, and A. Subic

School of Aerospace, Mechanical and Manufacturing Engineering
RMIT University, Melbourne, Australia

Abstract

Internal leakage, which has a significant impact on the efficiency and performance, is an inherent problem in the design of a twin-screw supercharger. The objective of this study is to understand the leakage flow mechanisms, and quantify the leaking rate through each leakage pathways in the supercharger. The numerical analysis is conducted using Computational Fluid Dynamics (CFD) software commercially available, FLUENT. The turbulent flow of an incompressible fluid is governed by the Reynolds-Averaged Navier-Stokes (RANS) equations. FLUENT solve the RANS equations over a finite volume grid. The Realizable k - ϵ turbulence model is employed because it has shown substantial improvements over the standard k - ϵ model where the flow features include strong streamline curvature, vortices, and rotation. Results show that the highest individual leakage occurs across the male and female rotor tip sealing lines, and the blowhole. Consequently, the improvements of a profile are concentrated on these two aspects.

1. Introduction

These days, the promotion of global environmental issues and resource saving efforts has been progressing rapidly worldwide. Particularly due to the popularity and influence of automotive engines, further achievement of low emissions and improvements in fuel consumption are quite urgent requirements in every region of the world. The solution to this problem is the addition of a power-boosting device to small engines. This can be achieved by using a twin-screw supercharger.

As shown in Figure 1, the twin-screw supercharger is a positive displacement compressor, the working cavity of which is enclosed by the casing bores, casing end plates and the helical surfaces of the male and female rotors. As the rotors rotate, the volume of the working cavity varies from zero to its maximum and from its maximum to zero periodically in a manner determined uniquely by the geometry of the supercharger. As a consequence of this periodic variation, the supercharger completes its suction, compression and discharge processes.

Due to the geometry of the mating parts and the need for clearances between rotors and casing, the supercharger has several leakage paths as follows: across the contact line between the male and female rotors, across the sealing lines between the rotor tips and casing, through the blowhole, and through the clearance between the end plate and the rotor end face at the discharge end.

Each leakage path has a different influence on the performance of the supercharger. It is very important to know the leakage through each leakage path and the percentage by which it can reduce the efficiencies for the purpose of prioritising design procedures in general and for improving the rotor lobe profile. The total number of papers published on twin-screw superchargers is not great when compared with the published work on certain common engineering components such as turbines or transformers, for example. Fong *et al.* [3] developed a mathematical procedure, which is proposed to calculate the inter-lobe clearance between two meshing screw rotors, and then represent the clearance

field by iso-clearance contour diagram (ICCD). Fleming and Tang [1] had a very detailed description on the leakage pathways analysis, and created a computer program in modeling of the flow in the leakage pathway. By means of the principle of mass conservation, the program calculated the leakage in every leakage pathway. Apart from Kovacevic *et al.* [4], there is hardly any reported activity in the use of CFD for twin-screw supercharger studies. In his paper, an advanced grid generation procedure was described. By its use and the inclusion of additional source terms and boundary conditions in the standard governing equations, heat and fluid flow within a twin-screw supercharger has been estimated by use of CFD solvers.

In this preliminary study, the contribution is focused on the analysis of leakage distribution by using the commercial CFD code FLUENT 6.0 [2].

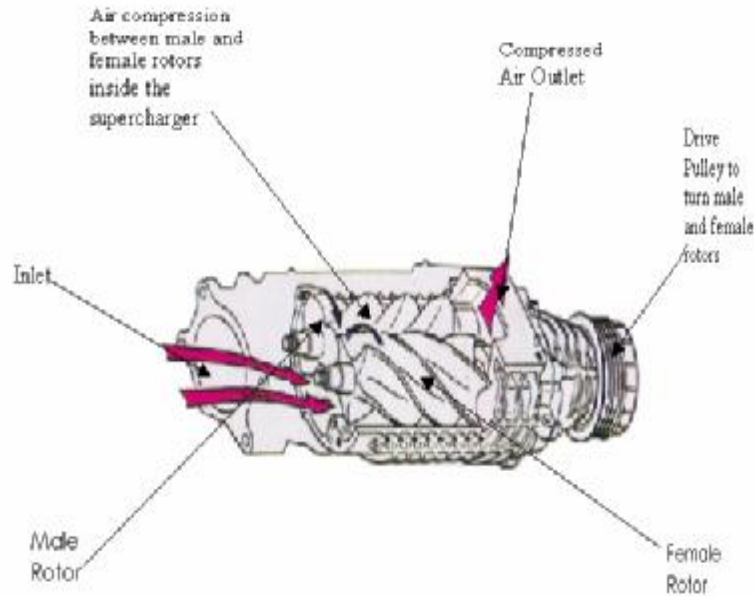


Figure 1. The twin-screw supercharger assembly

2. Theory

2.1. The governing equations

The governing equations for the turbulent incompressible flow encountered in this research are the steady-state RANS equations for the conservation of mass and momentum, which are present in the following forms [2]:

Continuity:

$$\frac{\partial}{\partial x_i} (\overline{ru_i}) = 0 \quad (1)$$

Momentum:

$$\frac{\partial}{\partial x_j} (\overline{ru_i u_j}) = -\frac{\partial \overline{p}}{\partial x_i} + \frac{\partial}{\partial x_j} \left[m \left(\frac{\partial \overline{u_i}}{\partial x_j} + \frac{\partial \overline{u_j}}{\partial x_i} - \frac{2}{3} d_{ij} \frac{\partial \overline{u_l}}{\partial x_l} \right) \right] + \frac{\partial}{\partial x_j} (-\overline{ru_i u_j}) \quad (2)$$

Here, r is density, \bar{p} is averaged pressure, m is the molecular viscosity and $-\overline{ru_i u_j}$ is the Reynolds stress. To correctly account for turbulence, Reynolds stresses are modelled in order to achieve closure of Equation (2). The method of modelling employed utilizes the Boussinesq hypothesis to relate the Reynolds stresses to the mean velocity gradients within the flow. Therefore, the Reynolds stresses are given by

$$-\overline{ru_i u_j} = m_t \left(\frac{\partial \bar{u}_i}{\partial x_j} + \frac{\partial \bar{u}_j}{\partial x_i} \right) - \frac{2}{3} \left(rk + m_t \frac{\partial \bar{u}_i}{\partial x_i} \right) \delta_{ij} \quad (3)$$

where m_t is the turbulent viscosity and k is the turbulent kinetic energy. For two-equation turbulence models, the turbulent viscosity is computed through the solution of two additional transport equations for the turbulent kinetic energy, and the turbulence dissipation rate.

2.2. The Realizable k - ϵ Model

In addition to the standard k - ϵ models, FLUENT also provides the so-called realizable k - ϵ model. The term "realizable" means that the model satisfies certain mathematical constraints on the normal stresses, consistent with the physics of turbulent flows [5].

The modelled transport equations for k and ϵ in the realizable k - ϵ model are

$$\frac{\partial}{\partial t}(rk) + \frac{\partial}{\partial x_i}(rku_j) = \frac{\partial}{\partial x_i} \left[\left(m + \frac{m_t}{s_k} \right) \frac{\partial k}{\partial x_j} \right] + G_k + G_b - re \quad (4)$$

$$\begin{aligned} \frac{\partial}{\partial t}(r\epsilon) + \frac{\partial}{\partial x_i}(r\epsilon u_j) = \frac{\partial}{\partial x_i} \left[\left(m + \frac{m_t}{s_e} \right) \frac{\partial \epsilon}{\partial x_j} \right] + rC_1 S \epsilon - \\ rC_2 \frac{\epsilon^2}{k + \sqrt{m\epsilon}} + C_{1\epsilon} \frac{\epsilon}{k} C_{3\epsilon} G_b \end{aligned} \quad (5)$$

In Equation (4) and (5), C_2 and $C_{1\epsilon}$ are constants, while C_1 is defined as

$$C_1 = \max \left[0.43, \frac{h}{h+5} \right] \text{ and } h = S \frac{k}{\epsilon} \quad (6)$$

In these equations, G_k represents the generation of turbulence kinetic energy due to the mean velocity gradient. G_b is the generation of turbulence kinetic energy due to buoyancy. s_k and s_e are the turbulent Prandtl numbers for k and ϵ , respectively. Similarly to the standard k - ϵ models, the turbulent viscosity is computed from

$$m_t = r C_m \frac{k^2}{\epsilon} \quad (7)$$

The difference between the realizable k - ϵ model and the standard k - ϵ model is that C_m is no longer constant. It is computed from

$$C_m = \frac{1}{A_0 + A_s \frac{kU^*}{\epsilon}} \quad (8)$$

where

$$U^* \equiv \sqrt{S_{ij}S_{ij} + \tilde{\Omega}_{ij}\tilde{\Omega}_{ij}}, \text{ and } \tilde{\Omega}_{ij} = \Omega_{ij} - 2e_{ijk}w_k, \quad \Omega_{ij} = \frac{1}{2} \left(\frac{\partial \bar{u}_i}{\partial x_j} - \frac{\partial \bar{u}_j}{\partial x_i} \right)$$

The model constants A_0 and A_s are given by

$$A_0 = 4.04, \quad A_s = \sqrt{6} \cos f$$

where

$$f = \frac{1}{3} \cos^{-1}(\sqrt{6}W), \quad W = \frac{S_{ij}S_{jk}S_{ki}}{\tilde{S}}, \quad \tilde{S} = \sqrt{S_{ij}S_{ij}}, \quad S_{ij} = \frac{1}{2} \left(\frac{\partial u_j}{\partial x_i} + \frac{\partial u_i}{\partial x_j} \right)$$

The constants applied in the realizable k - e model are listed below:

$$C_{1e} = 1.44, \quad C_2 = 1.9, \quad s_k = 1.0, \quad s_e = 1.2$$

3. Computational domain and mesh

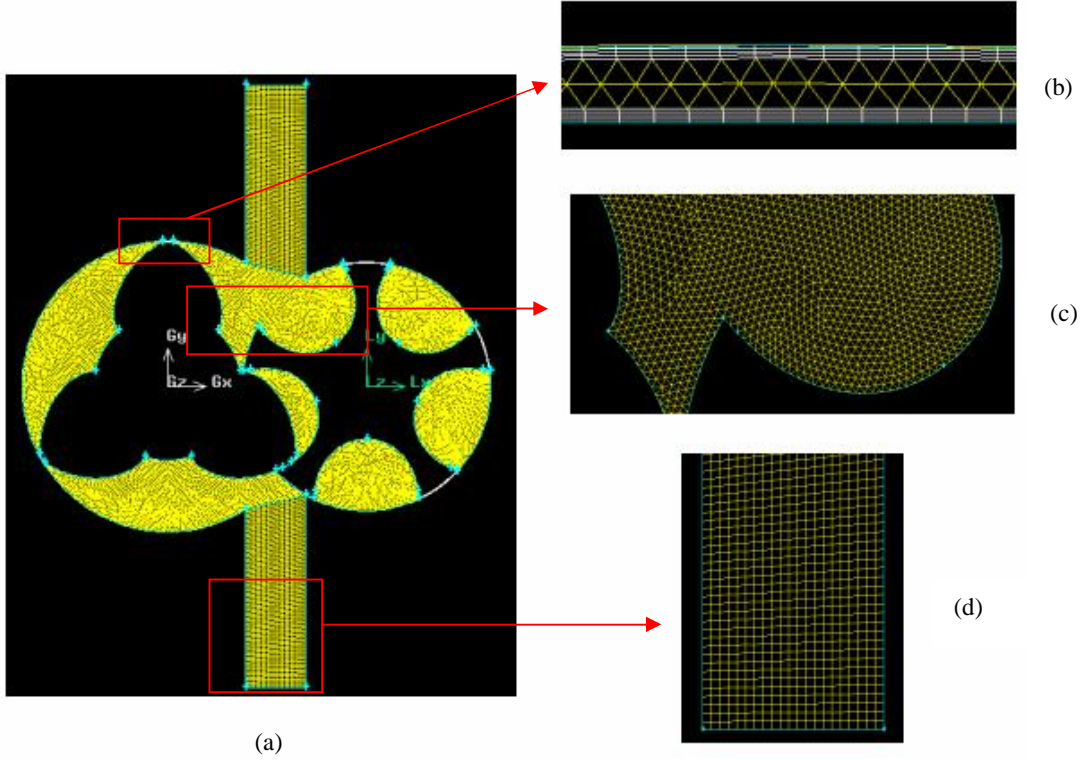


Figure 2. A meshed two-dimensional model of a supercharger

Figure 2(a) shows the two-dimensional model of a supercharger, which contains two rotors, casing, inlet and outlet. The flow area is meshed in different grid species in order to get more accurate simulation results and less computational time. As shown in Figure 2(b), the small clearance between the rotors and casing is meshed by very fine grid, since this area is the key part of the whole domain. Boundary layers are created along the walls and the tips of the rotors to accurately simulate the high velocity gradients at these locations. An unstructured mesh arrangement with triangle elements, as shown in Figure 2(c), is applied to the domain, which is around the rotors, because it contains

curves and corners. The locations of the inlet and outlet are placed far enough in order not to affect the flow in the casing. These two areas are created by a regular, structured grid of quadrilateral elements.

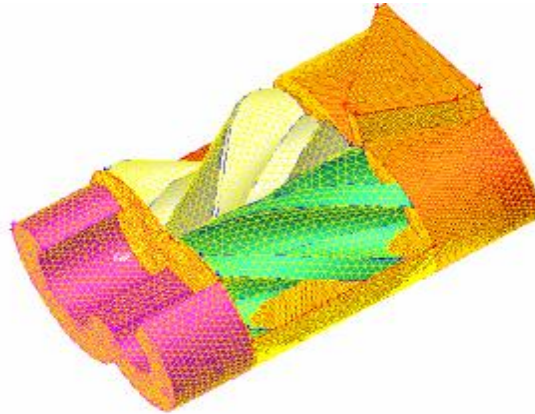


Figure 3. The three-dimensional mesh of a supercharger

In this study, the time required for mesh generation in three-dimensional for fluid analysis has been dramatically reduced through the use of tetra-mesh technology. Hexahedral mesh generally provides a higher degree of analysis accuracy than tetra-mesh for fluid analysis. However, analyses are not independent procedures like those seen with the conventional procedures, but a tool completely integrated in the entire development flow as evaluated from a macroscopic viewpoint. Because the emphasis is on making the generation of meshes much easier, a tetra-mesh is employed, as shown in Figure 3.

4. Results and discussion

4.1. CFD model verification

In this investigation, it is assumed that the leakage is independent of the flow induced by the rotor motion and that the leakage can be assessed by a steady flow at a series of rotor positions with a given pressure drop. Although FLUENT provides reasonable accuracy of the physical model, it still needs experimental results to validate the numerical results from our model. Apart from Fleming and Tang [2], there is hardly any reported research on leakage in twin-screw superchargers. In their paper, the leaking flow rates through each leakage path in the three-dimensional model are described.

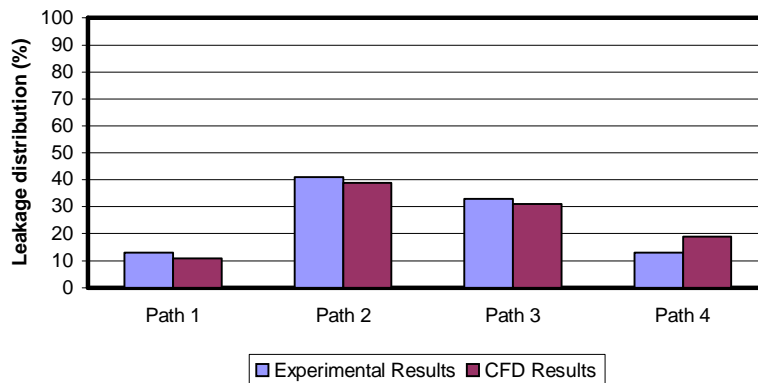


Figure 4. The comparison between experimental data and CFD results

By using the same boundary conditions, the predictions for each pathway individually from our model are compared with the experimental results from their paper. It seems probable that the models are overestimating the leakage through Path 4 and underestimating it through Paths 1, 2, and 3. However, comparison with test data shows the macro-predictions of the CFD models to be good.

4.2. Flow behaviors and results analysis in two-dimensional models

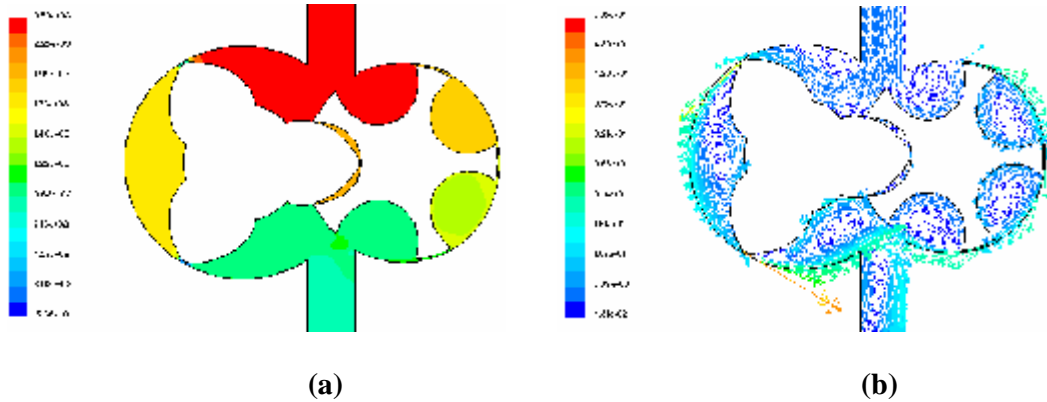


Figure 5. The pressure contours and velocity vectors of the 2D model

Figure 5 shows the pressure contours and velocity vectors of a two-dimensional model for a Sprintex supercharger. It can be seen clearly from Figure 5(a) that the pressure is high in the discharge area on the top, and low in the suction area on the bottom. Due to the pressure gradient between the two areas, the leakage flow passes through the clearance, which is between two rotors and rotor-casings, and returns to the suction area. Figure 5(b) presents that the highest velocity is between the male rotor and casing, which means the highest leakage rate, is in this domain.

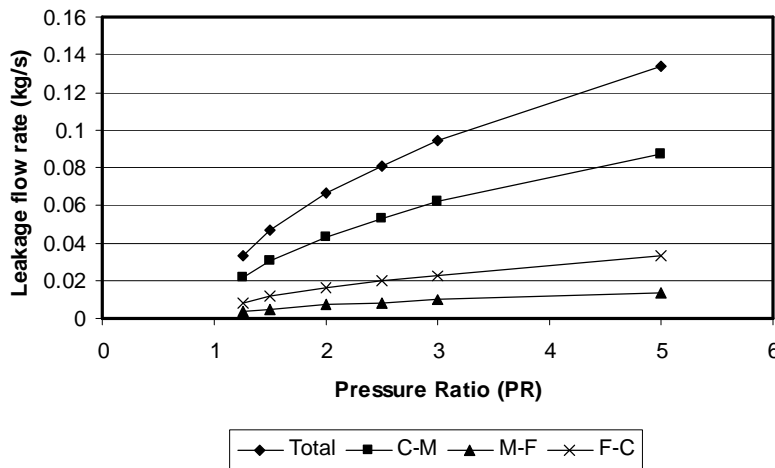


Figure 6. The leakage flow rate vs. PR in two-dimensional model

The internal leak in 2D model is determined by the three different clearances: between the casing and male rotor (C-M), between the two rotors (M-F), and between the female rotor and the casing (F-C). The leakage flow rate through the computational domain is studied as a function of the outlet/inlet pressure ratio (PR). The results show that the total leakage flow rate is proportional to the PR. Also, the leakage flow through every

location shows the same trend as the total flow rate, as shown in Figure 6. Although the leakage flow rate is proportional to the PR, the percentage leakage distribution at the three locations is independent of PR. For every PR, the leakage flow through three locations remains approximately constant. The highest leakage is between the casing and male rotor (C-M, 66%) followed by the female rotor and casing (F-C, 23%), and lastly between the male and female rotors (M-F, 11%).

4.3 Flow behaviors and results analysis in three-dimensional models

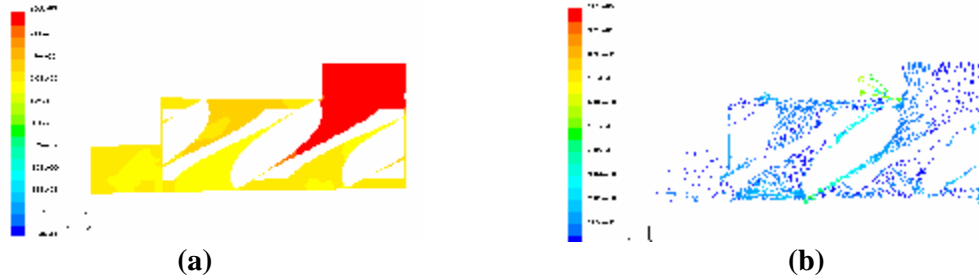


Figure 7. The pressure contours and velocity vectors in the axial cross-section of the 3D model for the Sprintex supercharger

In Figure 7, the pressure contours and velocity vectors in the axial cross-section of the 3D model are showed. It can be seen that low velocities are achieved not only in the working chamber but also in the suction and discharge ports, while the flow through the clearances changes rapidly and easily reaches high velocity. Table 1 gives the leakage flow rates through each leakage pathway in the Sprintex design. Again, Path 1 to Path 4 represent the leakage paths, which are the contact line between two rotors, the sealing lines between the rotor tips and the casing, the blowhole, and the clearance between the end plate and the rotor end face at the discharge end.

Table1. Leakage flow rates through each leakage pathway in the Sprintex design

Leakage pathways	Leakage flow rate (kg/s)	Leakage distribution (%)
Path 1	0.0015528	7.1
Path 2	0.0082927	37.8
Path 3	0.0065058	29.6
Path 4	0.0055924	25.5

The results of the leakage analysis show that Path 2 and Path 3 have a very important influence on the leakage distribution. To improve the performance of a supercharger by reducing the leakage through the different leakage paths, optimising the geometric parameters of a profile will be the most efficient method. Consequently, the improvement of a profile should concentrate on the following two aspects: reducing the blowhole area by an asymmetric profile, and reducing the leaking rates through Path 2 by increasing the wrap angle of the rotors.

4.4 Optimization

According to the above analysis, two improved profile have been developed from the definitions of the Sprintex profile design. By comparing the leakage flow rates between the Sprintex symmetric profile and the new asymmetric profile I, it is clear that the leakage flow rates do reduce in most pathways as well as in total value, although the

rate in Path 1 is increased due to the increasing of the contact line. There is a 1.4% reduction in the total leakage flow rate, while there is a 17% reduction in Path 3.

The comparison for the leakage flow rates between the Sprintex and the new symmetric profile II shows that the leakage flow rates do reduce in Path 2, as well as in total value, although the rate in Path 3 and Path 4 is increased slightly. There is a 1.5% reduction in total leakage flow rate, while there is a 7% reduction in Path 2.

5. Conclusions

In this study, a number of CFD models, including 2D and 3D, have been developed to analyse the leakage in a twin-screw supercharger. By using these models, the leakage flow rate through each leakage pathway has been quantified. The accuracy of the predictions for each pathway individually is obtained by comparing the CFD results with the experimental data available in the literature.

References

1. Fleming J.S., Tang Y., and Cook G., 1998, The twin helical screw compressor, Part 1: Development, applications and competitive position, Part 2: A mathematical model of the working process”, *Proceedings of the IMechEng, Journal of Mechanical Engineering Science*, Vol. 212, pp. 369.
2. FLUENT Incorporated, FLUENT 6.0 User’s Guide, 2001.
3. Fong Z.H., Huang F.C., and Fang H.S., 2001, Evaluating the inter-lobe clearance of twin-screw compressor by the iso-clearance contour diagram (ICCD), *Mechanism and Machine Theory*, 36 (2001) 725-742.
4. Kovacevic A., Stosic N., and Smith I.K., 2001, Analysis of screw compressor by means of three-dimensional numerical modeling”, *International Conference on Compressor and their System, IMechE Conference Transactions 2001-7*, London, pp.23-32.
5. Shih T.H., Liou W.W., Habbir A., and Zhu J., 1995, A new k - ϵ eddy-viscosity model for high Reynolds number turbulent flows - model development and validation, *Computers Fluids*, 24(3): 227-238.